Red death in *Caenorhabditis elegans* caused by *Pseudomonas aeruginosa* PAO1

Alexander Zaborin[a], Kathleen Romanowski[a], Svetlana Gerdes[b], Christopher Holbrook[a], Francois Lepine[c], Jason Long[a], Valeriy Poroyko[a], Stephen P. Diggle[d], Andreas Wilke[e], Karima Righetti[d], Irina Morozova[a], Trissa Babrowski[a], Donald C. Liu[a], Olga Zaborina[a,1], and John C. Alverdy[a,1,2]

[a]Department of Surgery, Pritzker School of Medicine, University of Chicago, Chicago, IL 60637; [b]Fellowship for Interpretation of Genomes, Burr Ridge, IL 60527; [c]INRS-Institut Armand-Frappier, 531 boul. Des Prairies, Laval, Quebec, Canada; [d]Centre for Biomolecular Sciences, University of Nottingham, Nottingham, NG7 2RD United Kingdom; and [e]Computation Institute, University of Chicago, Chicago, IL 60637

Edited by Frederick M. Ausubel, Harvard Medical School, Boston, MA, and approved March 6, 2009 (received for review December 25, 2008)

During host injury, *Pseudomonas aeruginosa* can be cued to express a lethal phenotype within the intestinal tract reservoir—a hostile, nutrient scarce environment depleted of inorganic phosphate. Here we determined if phosphate depletion activates a lethal phenotype in *P. aeruginosa* during intestinal colonization. To test this, we allowed *Caenorhabditis elegans* to feed on lawns of *P. aeruginosa* PAO1 grown on high and low phosphate media. Phosphate depletion caused PAO1 to kill 60% of nematodes whereas no worms died on high phosphate media. Unexpectedly, intense redness was observed in digestive tubes of worms before death. Using a combination of transcriptome analyses, mutants, and reporter constructs, we identified 3 global virulence systems that were involved in the ''red death'' response of *P. aeruginosa* during phosphate depletion; they included phosphate signaling (PhoB), the MvfR–PQS pathway of quorum sensing, and the pyoverdin iron acquisition system. Activation of all 3 systems was required to form a red colored PQS+Fe^{3+} complex which conferred a lethal phenotype in this model. When pyoverdin production was inhibited in *P. aeruginosa* by providing excess iron, red death was attenuated in *C. elegans* and mortality was decreased in mice intestinally inoculated with *P. aeruginosa*. Introduction of the red colored PQS+Fe^{3+} complex into the digestive tube of *C. elegans* or mouse intestine caused mortality associated with epithelial disruption and apoptosis. In summary, red death in *C. elegans* reveals a triangulated response between PhoB, MvfR–PQS, and pyoverdin in response to phosphate depletion that activates a lethal phenotype in *P. aeruginosa*.

pyoverdin | *P. aeruginosa* transcriptome | mice | phosphate depletion | PQS/Fe3+/rhamnolipid complex

Despite powerful antibiotics, *Pseudomonas aeruginosa* remains a leading cause of infection related mortality among hospitalized patients who are surgically injured or immunocompromised. Although traditionally considered to be primarily a lung pathogen, *P. aeruginosa* has been detected in the intestine of as many as 20% of normal subjects and up to 50% of hospitalized patients (1). Molecular typing of *P. aeruginosa* bloodstream infections has identified the intestinal tract to be the primary site from which *P. aeruginosa* disseminates and causes sepsis syndrome (2). Our ongoing work in this area has proposed that within the intestinal tract of a surgically injured host, colonizing strains of *P. aeruginosa* are directly activated to express a lethal phenotype by compounds released by host tissues. We have identified several of these compounds as immune elements (IFN-γ) (3), opioids (morphine, dynorphin) (4), and end-products of hypoxia (adenosine) (5), all of which are released into the intestinal tissues and lumen during surgical injury, ischemia, and inflammation.

The local concentration of extracellular phosphate is one of the multiple local environmental cues within the intestinal tract of a surgically injured host that might converge to activate a lethal phenotype in *P. aeruginosa*. Phosphate depletion is known to rapidly develop following major surgery and organ injury and independently predicts the development of lethal sepsis (6). We have recently documented that following surgical injury, phosphate becomes rapidly depleted within intestinal mucus to levels that are associated with the expression of important virulence determinants in *P. aeruginosa* (7). In surgically stressed mice, the expression of phosphosensor encoding gene *pstS* in intestinal *P. aeruginosa* was increased 32-fold while oral phosphate provision was associated with suppression of *pstS* and significantly attenuated mortality (7). We therefore hypothesized that within the intestinal tract, extracellular phosphate plays a major role in the mechanisms by which *P. aeruginosa* is cued to express a lethal phenotype. Here, using *P. aeruginosa* transcriptome analysis, *C. elegans*, *P. aeruginosa*, and mice model systems, we demonstrate that during phosphate depletion *P. aeruginosa* activates phosphate signaling (PhoB), the MvfR–PQS, and the pyoverdin iron acquisition systems and forms a red colored PQS+Fe^{3+} complex that confers a lethal phenotype in *C. elegans* and mice. These findings provide novel insight into the mechanisms by which *P. aeruginosa* is able to shift from an indolent colonizer to a lethal pathogen when present in the intestinal tract of a stressed host.

Results

Phosphate Depletion Shifts *P. aeruginosa* PAO1 to Express Lethality Against *C. elegans*. We used *P. aeruginosa* PAO1, a strain with attenuated killing ability against *C. elegans* when grown on nematode growth media (NGM) (8). To create bacterial lawns on which worms are feeding, we used standard NGM media that contains 25 mM potassium phosphate buffer (K-Ph) at pH 6.0 (NGM ↑ P_i) and compared it to NGM without the addition of K-Ph buffer (NGM ↓ P_i). Results indicated that phosphate depletion did not affect *C. elegans* when feeding on *Escherichia coli* lawns; however, it significantly decreased the progeny of *C. elegans* feeding on *P. aeruginosa* lawns (data not shown), suggesting that ↓ P_i activates virulence in *P. aeruginosa* rather than directly affects *C. elegans* viability. Next, we imposed starvation stress (prefasting *C. elegans* for 24 h before the ''point of transfer'' onto *P. aeruginosa* lawns). Prefasting caused up to 70% mortality at 50 h in nematodes feeding on *P. aeruginosa* NGM ↓ P_i lawns (Fig. 1*A*). We next imposed a period of heat shock stress (35 °C, 2 h) to nonfasting worms and found that heat

Author contributions: A.Z., S.P.D., O.Z., and J.C.A. designed research; A.Z., K. Romanowski, C.H., F.L., J.L., V.P., I.M., T.B., and O.Z. performed research; S.G., F.L., V.P., S.P.D., K. Righetti, D.C.L., O.Z., and J.C.A. contributed new reagents/analytic tools; A.Z., S.G., A.W., O.Z., and J.C.A. analyzed data; and A.Z., O.Z., and J.C.A. wrote the paper.

The authors declare no conflict of interest.

This article is a PNAS Direct Submission.

[1]O.Z. and J.C.A. contributed equally to this work.

[2]To whom correspondence should be addressed. E-mail: jalverdy@surgery.bsd.uchicago.edu.

This article contains supporting information online at www.pnas.org/cgi/content/full/0813199106/DCSupplemental.

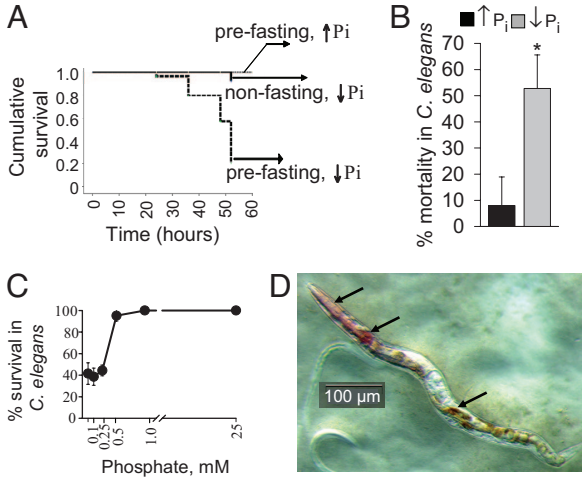

Fig. 1. Phosphate depletion shifts *P. aeruginosa* PAO1 to a lethal phenotype against *C. elegans*. (*A*) Kaplan-Meier surviving curves demonstrating mortality in nonfasted and prefasted nematodes. Data were analyzed using SPSS software employing the Long-rank (Mantel-Cox) test ($n = 40$/group, $P < 0.001$). (*B*) Mortality at 48 h in preheated *C. elegans* feeding on PAO1 NGM ↑ P_i and NGM ↓ P_i lawns. Data are mean ± SD ($n = 5$ plates, 10–12 worms/plate), $P < 0.001$ (Student's *t* test). (*C*) Mortality in prefasted *C. elegans* feeding on PAO1 lawns at varying phosphate concentration ($n = 40$/group, $P < 0.001$). (*D*) Appearance of redness in *C. elegans*. Image was created using the SZX16 Olympus stereomicroscope.

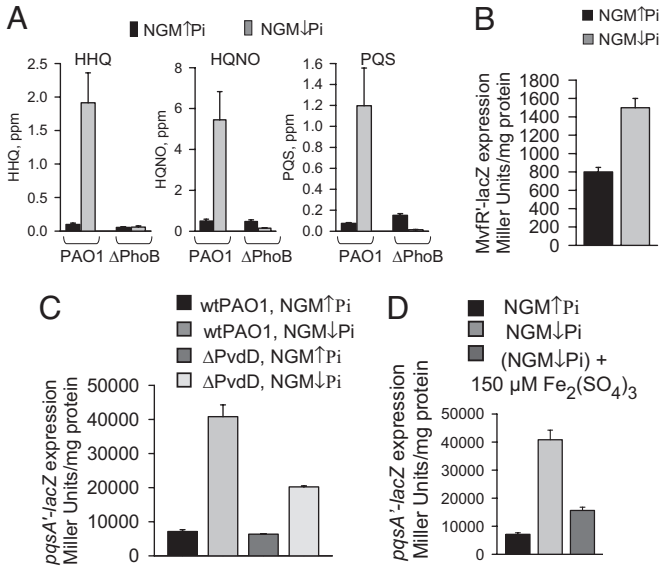

Fig. 2. The effect of phosphate depletion and iron supplementation on MvfR pathway in PAO1. Effect of phosphate depletion on (*A*) HHQ, HQNO, and PQS production in strains PAO1 and ΔPhoB, (*B*) on *mvfR′-lacZ* expression in PAO1/pGX1, and (*C*) *pqsA′-lacZ* expression in PAO1/pGX5 and ΔPvdD/pGX5 grown as lawns. (*D*) Effect of iron supplementation on *pqsA′-lacZ* expression in PAO1/pGX5. Data are mean ± SD ($n = 3$), $P < 0.001$ (Student's *t* test). Independent experiments were performed in triplicate and demonstrated similar results.

shock stress resulted in a similar mortality rate when worms fed on *P. aeruginosa* NGM ↓ P_i lawns (Fig. 1*B*). A threshold phosphate concentration of approximately 0.5 mM was identified below which *P. aeruginosa* PAO1 lethality was observed (Fig. 1*C*). Unexpectedly, red colored material was observed within the digestive tube of worms (Fig. 1*D*), the appearance of which predicted death. This phenomenon, herein termed "red death," was found in L1-L4, adult *C. elegans* and occasionally in eggs (Fig. S1). Characteristic features were the appearance of red spots in the pharynx with further distribution within the entire digestive tube. The appearance of redness followed by the development of mortality in *C. elegans* was found in worms subjected to both prefasting and heat stress suggesting that physiologic stress is required for "red death" to occur. Red death was reproducible with multiple *P. aeruginosa* PAO1 strains obtained from various laboratories (Fig. S2). The most rapid death developed within 2 hours where redness was initially observed within the vulva (Fig. S3). To define the role of bacterial vulva entry in this model, we performed reiterate experiments using the vulvaless mutant CB1309 genotype lin-2 (e1309). Results indicated that lin-2 (e1309) were highly susceptible to killing on *P. aeruginosa* lawns on NGM ↓ P_i with a mortality of approximately 40% at 4 h. All dying worms had the typical red color within their pharynx and digestive tubes, suggesting that vulva entry is not required for red death. To rule out the possibility that phosphate depletion resulted in increased feeding leading to a higher accumulation of *P. aeruginosa* in *C. elegans*, we tracked the intestinal accumulation of bacteria using the PAO1/EGFP strain (9). Results showed no differences in the accumulation of PAO1 within the digestive tubes of *C. elegans* (Fig. S4). Finally, to verify that phosphate depletion did not affect the life span of *C. elegans*, we performed experiments using sterile *C. elegans* pha-1(e2123). No statistical difference was found between the survival rates of the worms feeding on NGM ↑ P_i and NGM ↓ P_i *E. coli* OP50 lawns (Fig. S5).

Genome-Wide Transcriptome Analysis of *P. aeruginosa* Grown as Lawns on NGM ↓ P_i and NGM ↑ P_i. Transcriptome analyses of *P. aeruginosa* growing on NGM ↓ P_i versus NGM ↑ P_i demonstrated the expression of approximately 10% of genes to be changed >2.5-fold in response to P_i limitation; 323 genes were up-regulated and 229 were down-regulated (5.7% and 4.0% of the genome respectively). Depletion of phosphate led to the activation of a major phosphate signaling/uptake system PstS-PstCABD-PhoU-PhoB (10), multiple phosphate acquisition related genes, and genes associated with the alternative type II secretion (11) (Table S1). There was no up-regulation of genes associated with the type II and type III secretion systems during phosphate depletion (Table S2).

Despite the fact that *P. aeruginosa* lawns represent high cell density cells where quorum sensing (QS) is likely to be activated, P_i depletion induced an additional burst in the expression of genes associated with the QS regulon such as 4-hydroxy-2-alkylquinolines (HAQs), rhamnolipids, phenazines, cyanide, exotoxin A, and LasA protease (Table S3). It is noteworthy that increased biosynthesis of phenazines and hydroxy-2-alkylquinolines (each containing an aromatic moiety) were accompanied by pronounced (approximately ↓ 15-fold) repression of genes involved in degradation pathways of aromatic compounds (Table S3). Among the most up-regulated genes within the regulator core of the quorum sensing system were *mvfR* and MvfR-regulated *phnAB* and *pqsA-E* operons (4–8 fold), involved in the production of 4-hydroxy-2-heptylquinoline (HHQ), a precursor of the *Pseudomonas* quinolone signal (PQS) (12). This finding is in agreement with recently published data demonstrating that P_i limitation increases PQS production (13). Our data demonstrated a significant increase of HHQ, 2-heptyl-4-hydroxyquinoline N-oxide (HQNO), and PQS production on NGM ↓ P_i lawns. This response was completely abrogated in ΔPhoB mutant (Fig. 2*A*). Enhanced expression of *mvfR* under ↓ P_i was verified in PAO1/pGX1/*mvfR′-lacZ* strain (4) growing as lawn (Fig. 2*B*).

P_i limitation led to up-regulation of pyoverdin associated genes (*pa2384–2413*, *pa2418–2421*, and *pa2424–pa2428*)(Table S4). As pyoverdin biosynthesis is induced by iron limitation, we hypothesized that during ↓ P_i, pyoverdin might be required to

supply iron or to act as a direct signal to activate phosphate signaling pathways. To clarify this, we performed microarray analyses in pyoverdin mutant ΔPvdD grown as lawns on NGM ↓ P_i and NGM ↑ P_i, and observed a profound attenuation in the expression of genes associated with phosphate signaling and acquisition in response to ↓ P_i (Table S1). Similarly, *mvfR* and MvfR-regulated operons *pqsA-E* and *phnAB* were not up-regulated in the pyoverdin deficient mutant (Table S3). We confirmed this finding by measurement of *pqsA′-lacZ* expression in PAO1 and ΔPvdD harboring pGX5 plasmid (12) (Fig. 2*C*). Finally, we added excess iron to lawns to inhibit pyoverdin production and observed a similar attenuating effect on *pqsA* expression (Fig. 2*D*). We also noted in ΔPvdD compared to wtPAO1, higher expression of multiple phosphate-associated genes on high phosphate media (Table S1). These results suggested that pyoverdin is involved in the regulation of phosphate-related pathways in *P. aeruginosa*. Importantly, lack of pyoverdin in ΔPvdD resulted in a profound increase in the expression of genes associated with pyochelin biosynthesis (Table S4), further confirming a critical role for iron acquisition in the response to phosphate depletion.

Role of Phosphate Signaling, MvfR-PQS, and Iron Acquisition in Red Death. We performed experiments where *C. elegans* fed on NGM ↓ P_i lawns of *P. aeruginosa* mutants representative of each system: P_i signaling (ΔPstS and ΔPhoB); MvfR-PQS pathway of quorum sensing (ΔMvfR and double mutant ΔPqsAΔPqsH); and pyoverdin and pyochelin biosynthesis (ΔPvdD, ΔPchEF, and the double mutant ΔPvdDΔPchEF). In addition, we included ΔPhzA1 deficient in the biosynthesis of pyocyanin, a toxic redox-active compound produced in high amounts when PAO1 grows on NGM ↓ P_i agarized media (data not shown). Results demonstrated that compared to its wild type parental strain, ΔPstS had similar effect on *C. elegans* mortality, perhaps owing to the constitutive activation of *phoB* in ΔPstS (Fig. 3*A*). Consistent with this notion, ΔPhoB was avirulent against nematodes suggesting its critical role in the development of lethal phenotype in *P. aeruginosa*. Reiterative studies with ΔMvfR and ΔPqsAΔPqsH demonstrated that they did not induce redness and were non-lethal to *C. elegans*. Mortality and redness development with ΔPhzA1 was found to be similar to wtPAO1. However, since the expression of both operons *phzAG1* and *phzAG2* was up-regulated by P_i depletion (Table S3), we performed reiterative experiments using a double mutant ΔPhzAG1ΔPhzAG2 in which pyocyanin production is completely absent. Unexpectedly, ΔPhzAG1ΔPhzAG2 did not induce any redness in *C. elegans*, although it was highly lethal causing 80% mortality at 20 h (Fig. 3*B*). As an alternative to define the role of pyocyanin in red death, we added pure pyocyanin (Cayman Chemical) to ΔPhzAG1ΔPhzAG2 to a final concentration of 100 μM. Results demonstrated that the addition of pyocyanin to ΔPhzAG1ΔPhzAG2 did not induce redness and did not affect *C. elegans* mortality (Fig. 3*B*). Taken together, these data preclude us from establishing a definitive role of pyocyanin in red death. The striking lethality of ΔPhzAG1ΔPhzAG2 remains to be determined.

ΔPvdD was significantly attenuated in lethality against *C. elegans* (Fig. 3*A*), although it still induced mortality, perhaps as a result of up-regulation of other iron scavenging systems such as pyochelin (Table S4). However, in the presence of pyoverdin, pyochelin was not required for *P. aeruginosa* lethality against *C. elegans* as ΔPchEF caused mortality similar to wtPAO1 (Fig. 3*A*). The observation that ΔPvdDΔPchEF was completely nonlethal against *C. elegans* provided further evidence that the ability of *P. aeruginosa* to obtain iron is required to produce red death in *C. elegans*.

We next hypothesized that pyoverdin production increases the amount of iron in *P. aeruginosa*, which then binds to PQS. As it

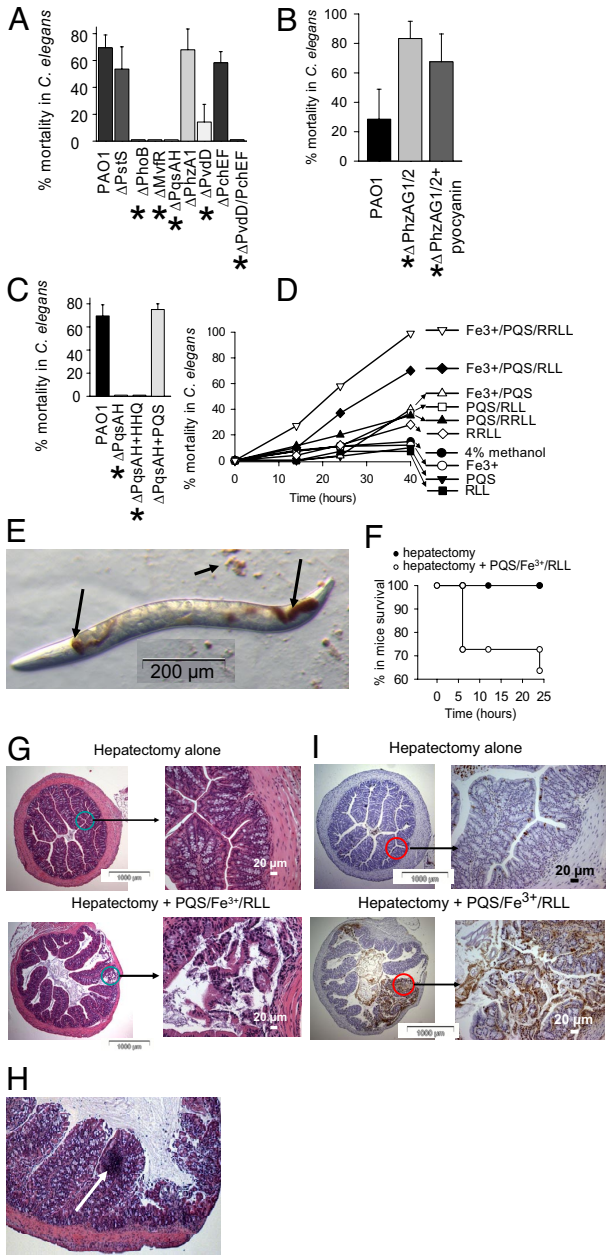

Fig. 3. Effect of PQS/Fe^{3+}/rhamnolipids complex on mortality in *C. elegans* and mice. (*A*) Mortality at 48 h in prefasted *C. elegans* feeding on NGM ↓ P_i lawns of *P. aeruginosa* mutants, n = 8/plate, 5 plates/variant. Mutants labeled with * do not induce redness development in *C. elegans*. (*B*) Mortality at 24 h prefasted *C. elegans* feeding on NGM ↓ P_i lawns of ΔPhzAG1ΔPhzAG2 (ΔPhzAG1/2) mutant. Pyocyanin supplementation does not affect mortality and does not restore redness development, n = 8/plate, 5 plates/variant. (*C*) PQS supplementation restores mortality in prefasted *C. elegans* feeding on NGM ↓ P_i lawns of ΔPqsAΔPqsH (ΔPqsAH). (*D*) Mortality in prefasted *C. elegans* feeding on artificial lawns. n = 8/plate, 5 plates/variant. Independent experiments were performed in triplicate and demonstrated similar results. (*E*) Image of nematode feeding on abiotic lawn containing PQS/Fe^{3+}/RLL. (*F*) Mortality in mice subjected to 30% hepatectomy coupled with direct injection of 200 μl of PQS/Fe^{3+}/RLL into cecum. n = 5 per group in 2 independent experiments. (*G*) Histology (H&E staining) of intestinal sections in mice killed at 6 h. (*H*) Site of inflammatory cell accumulation (shown by arrow). (*I*) TUNEL assay of intestinal sections in mice killed at 6 h.

is known that PQS can form a red PQS-Fe^{3+} complex (14), we hypothesized that red death develops as a result of the formation of this complex. To confirm this, we first verified the critical role

for PQS in red death. We allowed *C. elegans* to feed on lawns of the double mutant ΔPqsAΔPqsH (deficient in PQS and HHQ) supplemented with exogenous PQS or HHQ (40 μM). ΔPqsAΔPqsH cannot convert HHQ to PQS allowing for the role of PQS to be defined in these experiments. Results demonstrated that the addition of PQS, but not HHQ, restored both redness (Fig. S6) and mortality in *C. elegans* feeding on ΔPqsAΔPqsH NGM ↓ P_i lawns (Fig. 3*C*). We further hypothesized that the PQS/Fe^{3+} moiety itself is toxic to *C. elegans*. To test this, we created artificial lawns consisting of boiled *E. coli* cells in solutions of PQS alone, iron alone, PQS/Fe^{3+}, as well as combinations of each with mono- (RLL) and di-rhamnolipids (RRLL), compounds that have been recently shown to solubilize PQS and enhance its biological activity (15). Further justification for this approach was the observation that genes associated with rhamnolipid biosynthesis were increased up to 12-fold under ↓ P_i (Table S3). We used mono- and di-rhamnolipids that differ in their chemotactic response on *P. aeruginosa* (16). Red spots were visible on all lawns containing the PQS/Fe^{3+} moiety and within the digestive tubes of *C. elegans* feeding on these lawns (Fig. 3*E*). The combination of PQS+Fe^{3+} with rhamnolipids had the highest lethal effect against *C. elegans* (Fig. 3*D*). Neither PQS, nor iron, nor RLL alone had any effect on mortality.

PQS/Fe^{3+}/Rhamnolipid Complex Induces Lethality When Introduced into the Intestine of Mice. To determine if the PQS/Fe^{3+}/RLL(RRLL) kills mice when present in the intestine, we injected it into the cecum of mice subjected to a surgical stress (30% hepatectomy). PQS/Fe^{3+}/RLL mixture caused 30% mortality in mice at 6 h (Fig. 3*F*), and mice developed signs of severe sepsis including lethargy, ruffled fur, and shivering. Hematoxylin and eosin staining of intestinal tissues (cecum) from moribund mice killed at 6 h revealed visible epithelial cell disruption (Fig. 3*G*), localized areas of inflammatory cell accumulation (Fig. 3*H*), and epithelial apoptosis (Fig. 3*I*). When reiterative experiments were performed with PQS and rhamnolipids alone no mortality or epithelial cell disruption was observed. The effect of the PQS mixtures containing RLL did not differ from those containing RRLL.

Exogenous PQS Induces Pyoverdin Production, However It Does Not Play a Role as the Initial Trigger Under ↓ P_i. We next hypothesized (Fig. S7*A*) that the mechanism by which ↓ P_i enhances pyoverdin production involves iron depletion caused by PQS binding of iron—a finding that has been recently demonstrated by several investigators (14, 17, 18). We performed experiments to verify this hypothesis. When bacteria are seeded onto agarized NGM media they likely consume iron in the agar along a concentration gradient, thus making the precise amount of iron to which bacteria are exposed difficult to define. Therefore, experiments were performed in liquid NGM ↑ P_i and NGM ↓ P_i media where the iron concentration was determined to be below a detectable level <2 μM. Since phosphate itself can chelate Fe^{3+} (19), and as such approximately 0.5 μM iron will be removed with the K-Ph buffer, we added 0.5 μM iron to the NGM ↓ P_i media (similar to the procedure we used to prepare NGM ↓ P_i agarized media). We found that the pyoverdin production was rapidly increased in NGM ↓ P_i (Fig. S7*B*). We further supplemented NGM ↓ P_i media with 25 mM KCl and maintained pH 6.0 by adding 25 mM Mes buffer, pH 6.0. These manipulations did not abrogate the effect of phosphate depletion on pyoverdin production (Fig. S7*C*). The addition of PQS led to a rapid increase in pyoverdin production in NGM ↓ P_i media (Fig. 4*A*). To further verify the role of PQS on pyoverdin production, pyoverdin was measured in the PQS deficient mutant ΔPqsAΔPqsH. To our surprise, this mutant produced pyoverdin in response to ↓ P_i similar to that of wtPAO1 (Fig. 4*B*) suggesting that PQS is not an initial trigger. We next defined the dose dependency of

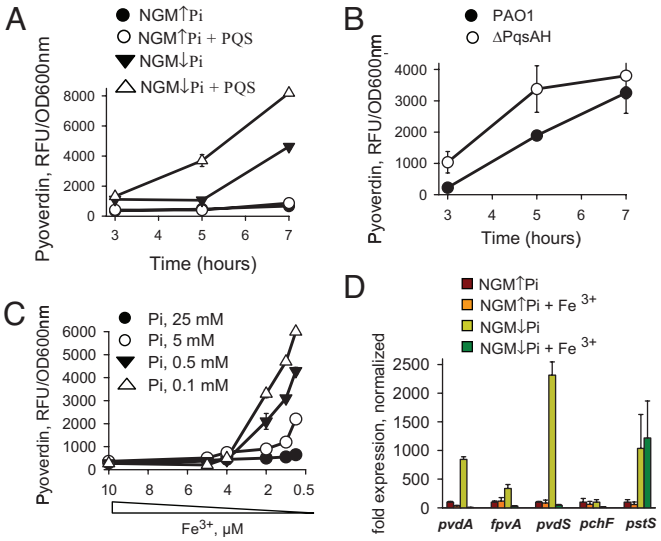

Fig. 4. Role of phosphate on the activation of pyoverdin system in *P. aeruginosa* PAO1. (*A*) Effect of exogenous PQS, 40 μM on pyoverdin production by *P. aeruginosa* PAO1 grown in NGM ↓ P_i and NGM ↑ P_i liquid media. (*B*) Production of pyoverdin in PAO1 and its derivative mutant ΔPqsAH grown in NGM ↓ P_i liquid media. (*C*) Dose dependent effect of $Fe_2(SO_4)_3$ on pyoverdin production at varying concentrations of K-Ph buffer added to NGM ↓ P_i while keeping pH constant at 6.0 with 25 mM Mes buffer. (*D*) Expression of phosphate (*pstS*) and iron (*pvdA*, *fpvA*, *pvdS*, *pchF*) related genes in *P. aeruginosa* PAO1 grown in NGM ↓ P_i and NGM ↑ P_i liquid media with or without supplementation of 10 μM Fe^{3+}.

phosphate on pyoverdin production by adding varying concentrations of K-Ph buffer to NGM ↓ P_i while keeping the pH 6.0 using 25 mM Mes and found the highest production of pyoverdin at $[P_i] \leq 1$ mM (Fig. S7*D*). Reiterative experiments were performed using a conventionally defined phosphate media described by Hancock and coworker (20) which demonstrated similar results (data not shown). We next found that phosphate concentration affects the level at which iron depletion increases pyoverdin production (Fig. 4*C*). At high doses of phosphate, pyoverdin production in *P. aeruginosa* barely responded to iron depletion. For completeness, we measured the expression of genes associated with phosphate (*pstS*) and iron (*pvdA*, *fpvA*, *pvdS*, *pchF*) using qRT-PCR array. As seen in Fig. 4*D*, iron limitation induced the expression of pyoverdin associated genes (*pvdA*, *fpvA*, *pvdS*) at ↓ P_i but not at ↑ P_i. Phosphate limitation did not influence the expression of the pyochelin associated gene *pchF*.

Excess Iron Attenuates Red Death in *C. elegans* and Decreases Mortality in Mice. To define the roles of extracellular iron and phosphate in a clinical context, we used an animal model of gut-derived sepsis developed in our laboratory that recapitulates surgical injury and lethal sepsis due to intestinal *P. aeruginosa* (21). In this model, phosphate becomes depleted in the distal tract intestinal mucus at levels of <0.1 mM (7). Similarly, we measured iron in the distal intestinal mucus 24 h following 30% hepatectomy and discovered it to be decreased by 50% (Fig. 5*A*). To determine the relative contribution of iron on *P. aeruginosa* lethality in this model, iron was added to the *P. aeruginosa* inoculums before their injection into the intestine. Results demonstrated that local intestinal supplementation with high concentrations of iron significantly attenuated mortality in mice (Fig. 5*B*). Finally, we performed complementary experiments in the *C. elegans* model and demonstrated a similar protective effect of iron on *C. elegans* mortality when worms fed on *P. aeruginosa* growing on NGM ↓ P_i (Fig. 5*C*).

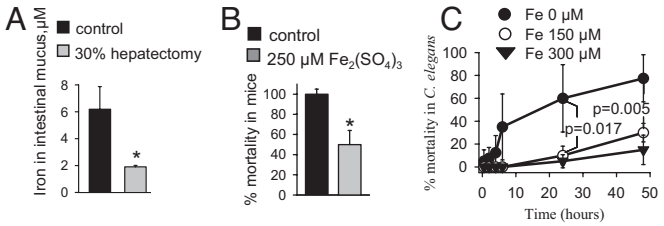

Fig. 5. Excess iron attenuates the lethality of *P. aeruginosa* PAO1 in animal models. (*A*) Depletion of iron in intestinal mucus of mice subjected to 30% hepatectomy. $n = 5$ per group in 2 independent experiments, $P < 0.05$. (*B*) Supplementation of *P. aeruginosa* with 250 μM $Fe_2(SO_4)_3$ significantly attenuates mortality in mice. $n = 10$/group in 2 independent experiments. (*C*) Supplementation of *P. aeruginosa* with 150 or 300 μM Fe^{3+}significantly attenuates mortality in prefasted *C. elegans* feeding on NGM $\downarrow P_i$ *P. aeruginosa* lawns. $n = 40$/group in 2 independent experiments.

Discussion

Evidence continues to demonstrate that the gastrointestinal tract and its microbiota play a major role in the development of sepsis during critical illness and after major traumatic injury. In this regard, *P. aeruginosa* is among the most common nosocomial pathogens to cause lethal sepsis from the intestinal tract following burn injury, major surgery, and bone marrow transplantation (22). Based on results from the present study, phosphate depletion may represent a previously unappreciated environmental cue in the intestinal tract of severely injured and physiologically stressed patients that has a major influence on *P. aeruginosa* lethality. A better understanding of how *P. aeruginosa* senses and responds to phosphate depletion within the intestinal microenvironment is critical for the development of strategies to contain this pathogen which continues to be among the most antibiotic resistant organisms infecting hospitalized patients.

Data from the present study provide compelling evidence that phosphate depletion induces virulence systems in *P. aeruginosa* associated with phosphate, quorum sensing, and iron signaling. MvfR-regulated biosynthesis of quinolone signaling molecules appeared to play a major role in the response of *P. aeruginosa* to phosphate depletion. In the present study, up-regulation of *mvfR* was found to be PhoB-dependent. Specific DNA sequences (*pho* boxes) where PhoB binds to and activates the transcription of its regulated genes have been previously located upstream of genes encoding 3 main quorum sensing transcriptional regulators, LasR, RhlR, and MvfR (13). However in the present study only *mvfR* and MvfR-regulated genes were found to be up-regulated in PAO1 growing as lawns on $\downarrow P_i$ media. The finding that MvfR is regulated by PhoB and that both are required for *C. elegans* mortality was not unexpected as the PhoB box is located within the regulatory region of MvfR (13). However the finding that activation of PhoB-MvfR during phosphate depletion was nearly completely inhibited in the pyoverdin deficient mutant ΔPvdD, reveals a novel mechanism of interconnectedness of these systems when responding to low phosphate conditions. The impact of pyoverdin on the lethality of *P. aeruginosa* appears to be dependent on both its ability to scavenge iron and its possible role as a signaling molecule involved in phosphate-signaling related pathways. Yet precisely how phosphate depletion increases pyoverdin production remains unclear. In the present study, we tested the hypothesis that increased PQS during phosphate depletion resulted in iron depletion as PQS is known to chelate iron (14). As suggested, iron chelating by PQS results in iron depletion which in turn increases pyoverdin production (17). However, since the PQS deficient mutant produced the same level of pyoverdin as the wtPAO1, we surmised that PQS is not the initial trigger of pyoverdin activation under $\downarrow P_i$. Thus the mechanism by which phosphate depletion increases pyoverdin production remains to be elucidated. The importance of understanding the interplay between iron and phosphate has broad implications as the finding that phosphate depletion alters iron homeostasis has also been described in *Sinorhizobium meliloti* (23) and *Arabidopsis* plants (24) and, as such, appears to be conserved across species and kingdoms.

The finding in the present study that the combination of PQS, Fe^{3+}, and rhamnolipids kills *C. elegans* and mice provides a novel mechanism by which *P. aeruginosa* may kill its host and further supports an important interplay between phosphate, iron, and quorum sensing in a low phosphate environment. The development of the artificial lawns consisting of heat-killed *E. coli* with PQS, iron, and rhamnolipids provides a unique opportunity to order and more completely understand how this combination causes death. Future studies aimed at performing transcriptome analyses of *C. elegans* exposed to the various combinations of these components will allow for a more complete understanding of this novel observation.

In summary, when *P. aeruginosa* colonizes the intestinal tract during injury or physiologic stress, there appears to be a fragile balance between bacterial mutualism and opportunism that may be significantly influenced by the local concentration of phosphate, a cue that may function as a proxy for host health status. Appreciation of such a subtle mechanism in pathogens that colonize the intestinal tract of critically ill patients has important implications for the design of phosphorylated compounds that might molecularly silence *P. aeruginosa* and other pathogens from expressing a lethal phenotype when present in this hostile and nutrient scarce environment.

Materials and Methods

Nematodes. *Caenorhabditis elegans* strains N2 and GE24 pha-1 (e2123), which produce dead embryos at 25 °C, and CB1309 genotype lin-2 (e1309) vulvaless mutant were obtained from the *Caenorhabditis* Genetics Center (http://www.cbs.umn.edu/CGC/). Egg preparation for synchronization, and transferring were performed accordingly to the ''Maintenance of *C. elegans*'' (http://www.wormbook.org/chapters/www_strainmaintain/strainmaintain.html). *E. coli* OP50 and *P. aeruginosa* PAO1 were grown overnight on agarized Luria Broth (LB) and Tryptic Soy Broth (TSB), respectively. Bacterial cells were then harvested from plates, suspended in PBS (OD 600 nm ≈1.0), and 100 μl was dropped onto NGM $\uparrow P_i$ plates. For phosphate depletion experiments, bacteria collected from plates were suspended in 10% glycerol. We specifically chose 2 different solutions in which to prepare bacterial suspensions to completely eliminate phosphate (10% glycerol) or maintain a high level of phosphate (PBS) at all steps of the experiments. We chose 10% glycerol to prevent osmotic shock. Plates were incubated at 37 °C for 24 h and then for an additional approximately 20 h at room temperature. Adult *C. elegans* were transferred from *E. coli* OP50 lawns onto NGM $\uparrow P_i$ and NGM $\downarrow P_i$ lawns. The plates were seeded with 8–12 worms in 5 replicates per trial performed.

For prefasting, nematodes were seeded onto *E. coli* NGM $\uparrow P_i$ plates for approximately 20–25 h after bacterial lawns appeared consumed.

For heat shock stress, nematodes on *E. coli* NGM $\uparrow P_i$ plates were subjected to 2 h incubation at 35 °C. After heating, plates with worms were adjusted to 25 °C during 1 h, followed by transferring worms onto PAO1 NGM $\uparrow P_i$ and NGM $\downarrow P_i$ lawns.

(NGM $\downarrow P_i$) was created by excluding potassium phosphate (K-Ph) buffer from NGM protocol (NGM protocol: agar, 17 g/L (Fisher); peptone, 2.5 g/L (Sigma); cholesterol, 5 mg/L (Sigma); NaCl, 3 g/L; $MgSO_4$, 1 mM; $CaCl_2$, 1 mM; potassium phosphate buffer (K-Ph), 25 mM, pH 6.0 [prepared from 1M monobasic solution (Sigma) and 1M dibasic solution (Sigma); ampicillin, 40 mg/L in experiments with *P. aeruginosa*]. Since the removal of K-Ph buffer shifted the pH from 6.0 to 6.7, the pH of NGM $\downarrow P_i$ was adjusted with 0.2 N HCl. We also found that 1M K-Ph buffer pH 6.0 contains approximately 20–28 μM of elemental iron thus contributing 0.5–0.7 μM of iron to NGM $\uparrow P_i$ liquid media. Therefore, NGM $\downarrow P_i$ media was supplemented with $Fe_2(SO_4)_3$ to add back iron removed with the phosphate buffer. In specific experiments, 25 mM KCl and/or 25 mM Mes buffer, pH 6.0, were added to NGM $\downarrow P_i$ media. To ensure that internal hatching was not a cause of red death, reiterative experiments were performed with *C. elegans* strain GE24 pha-1 (e2123) that produce dead embryos at 25 °C.

Genome-Wide Transcriptome Analysis. All samples for gene expression analysis were prepared from biological triplicates. *P. aeruginosa* cells of PAO1 and ΔPvdD mutant, both obtained from P. Cornelis were collected from lawns grown on NGM ↑ P_i and NGM ↓ P_i plates directly in the RNA protect buffer (Qiagen), and RNA isolation and DNA degradation were performed as previously described (4). RNA was concentrated by precipitation with ethanol followed by dissolving in RNase-free water to at final concentration of ≥2 μg/μl. Microarray analysis was accomplished using Affymetrix *P. aeruginosa* GeneChips (Affymetrix) at the University of Chicago Functional Genomics Facility; RNA quality, quantity, and DNA contamination were determined with an Agilent Bioanalyzer 2100 (Agilent Technologies). The absence of DNA contamination was verified by PCR analysis. The cDNA preparation and hybridization were carried out as described in the Affymetrix GeneChip Expression Analysis Manual for *P. aeruginosa* RNA samples. The GeneChip Operating Software (GCOS) was used for detection of signal intensities. All signals were scaled according to GCOS default target signal value 500. Invariant set normalization was performed using dchip2006 (Affymetrix). The PM-only model was used to generate gene signal intensities. Dchip was used for identification of differentially expressed genes. Thresholds for selecting significant genes were set at a relative difference >1.2-fold and absolute intensity differences between experimental samples and baseline samples >100 and *t* test $P < 0.05$. Genes that met the criteria simultaneously were considered to represent significant changes. Microarray data were analyzed within the metabolic and genomic context provided by the SEED database (http://www.theSEED.org/) and the *Pseudomonas* Genome Database (http://www.*Pseudomonas*.com/).

Creation of Artificial Lawns for Nematodes *C. elegans*. We first determined that a concentration of 1.5 mM PQS mixed with ferric sulfate at molar ratio of 3:1 (PQS:Fe) was needed to reproduce the red coloration seen in *C. elegans* experiments. The concentration of rhamnolipids (1.4 mM) was chosen based on preliminary experiments in which we determined their highest nonlethal dose in *C. elegans*. To create artificial lawns, *E. coli* OP50 grown in LB were adjusted to $OD_{600\ nm}$ approximately 1.2, aliquoted in 600 μl, boiled for 15 min, and centrifuged at 5,000 rpm, for 5 min. Pellets from each 600 μl aliquots were resuspended in 100 μl of mixtures containing (*i*) H_2O plus 4 μl of methanol, (*ii*) 2.5 μl of 10 mM $Fe_2(SO_4)_3$, (*iii*) 4 μl of PQS, or (*iv*) 2.5 μl of (10 mM $Fe_2(SO_4)_3$ + 4 μl PQS) and pooled onto agarized plates containing 1.7% agar in water. To prepare the mixtures with rhamnolipids, 35 μl of (RLL) or 100 μl of (RRLL) in small wells were evaporated at room temperature, and 100 μl of prepared *E. coli* mixtures were added to wells, mixed, and pooled onto agarized plates. Fasting *C. elegans* were transferred onto the artificial lawns and dynamically tracked for mortality at 23 °C. PQS, 40 mM methanol solution, RLL, 2020 ppm methanol solution, and RRLL, 630 ppm methanol solution were prepared as previously described (16, 25).

Statistical Analysis. Statistical analysis was performed with Student's *t* test using Sigma plot software, and Kaplan-Maier survival graphs using SPSS software. Cutoff based Fisher's Exact Test (based on the hypergeometric distribution) and noncutoff based Maxmean NR methods were used to compute *p*-values for gene sets in microarray data.

Bacterial strains; mouse model of gut-derived sepsis; TUNEL assay; H&E staining; HHQ, HQNO, and PQS quantification; pyoverdin assay; iron assay; Q-RT PCR; β-galactosidase assay; lifespan of nematodes; and Pyocyanin, PQS, and HHQ supplementations to *P. aeruginosa* mutant lawns are presented in *SI Materials and Methods*.

ACKNOWLEDGMENTS. We thank Dr. R. Hancock for providing ΔPhoB mutant; Dr. P. Cornelis for providing ΔPvdD, ΔPchEF, and ΔPvdD/ΔPchEF mutants; and M. Camara and P. Williams for providing ΔPhzAG1ΔPhzAG2 mutant. This work was supported by National Institutes of Health R01 GM62344–09 (J.A.), Charles B. Huggins Research Award (O.Z.), Royal Society (S.P.D.), and MEST-CT-2005–020278 Antibiotarget (K. Righetti).

1. Thuong M, et al. (2003) Epidemiology of Pseudomonas aeruginosa and risk factors for carriage acquisition in an intensive care unit. *J Hosp Infect* 53:274–282.
2. Murono K, Hirano Y, Koyano S, Ito K, Fujieda K (2003) Molecular comparison of bacterial isolates from blood with strains colonizing pharynx and intestine in immunocompromised patients with sepsis. *J Med Microbiol* 52:527–530.
3. Wu L, et al. (2005) Recognition of host immune activation by Pseudomonas aeruginosa. *Science* 309:774–777.
4. Zaborina O, et al. (2007) Dynorphin activates quorum sensing quinolone signaling in Pseudomonas aeruginosa. *PLoS Pathog* 3:e35.
5. Patel NJ, et al. (2007) Recognition of intestinal epithelial HIF-1alpha activation by Pseudomonas aeruginosa. *Am J Physiol Gastrointest Liver Physiol* 292:G134–G 142.
6. Shor R, et al. (2006) Severe hypophosphatemia in sepsis as a mortality predictor. *Ann Clin Lab Sci* 36:67–72.
7. Long J, Zaborina O, Holbrook C, Zaborin A, Alverdy J (2008) Depletion of intestinal phosphate after operative injury activates the virulence of P aeruginosa causing lethal gut-derived sepsis. *Surgery (St Louis)*144:189–197.
8. Lee DG, et al. (2006) Genomic analysis reveals that Pseudomonas aeruginosa virulence is combinatorial. *Genome Biol* 7:R90.
9. Wu L, et al. (2004) High-molecular-weight polyethylene glycol prevents lethal sepsis due to intestinal Pseudomonas aeruginosa. *Gastroenterology* 126:488–498.
10. Monds RD, Newell PD, Schwartzman JA, O'Toole GA (2006) Conservation of the Pho regulon in Pseudomonas fluorescens Pf0–1. *Appl Environ Microbiol* 72:1910–1924.
11. Ball G, Durand E, Lazdunski A, Filloux A (2002) A novel type II secretion system in Pseudomonas aeruginosa. *Mol Microbiol* 43:475–485.
12. Xiao G, et al. (2006) MvfR, a key Pseudomonas aeruginosa pathogenicity LTTR-class regulatory protein, has dual ligands. *Mol Microbiol*
13. Jensen V, et al. (2006) RhlR expression in Pseudomonas aeruginosa is modulated by the Pseudomonas quinolone signal via PhoB-dependent and -independent pathways. *J Bacteriol* 188:8601–8606.
14. Bredenbruch F, Geffers R, Nimtz M, Buer J, Haussler S (2006) The Pseudomonas aeruginosa quinolone signal (PQS) has an iron-chelating activity. *Environ Microbiol* 8:1318–1329.
15. Calfee MW, Shelton JG, McCubrey JA, Pesci EC (2005) Solubility and bioactivity of the Pseudomonas quinolone signal are increased by a Pseudomonas aeruginosa-produced surfactant. *Infect Immun* 73:878–882.
16. Tremblay J, Richardson AP, Lepine F, Deziel E (2007) Self-produced extracellular stimuli modulate the Pseudomonas aeruginosa swarming motility behaviour. *Environ Microbiol* 9:2622–2630.
17. Diggle SP, et al. (2007) The Pseudomonas aeruginosa 4-quinolone signal molecules HHQ and PQS play multifunctional roles in quorum sensing and iron entrapment. *Chem Biol* 14:87–96.
18. Royt PW, et al. (2007) Iron- and 4-hydroxy-2-alkylquinoline-containing periplasmic inclusion bodies of Pseudomonas aeruginosa: A chemical analysis. *Bioorg Chem* 35:175–188.
19. Rasmussen L, Toftlund H (1986) Phosphate compounds as iron chelators in animal cell cultures. *In Vitro Cell Dev Biol* 22:177–179.
20. Poole K, Hancock RE (1984) Phosphate transport in Pseudomonas aeruginosa. Involvement of a periplasmic phosphate-binding protein. *Eur J Biochem* 144:607–612.
21. Alverdy J, et al. (2000) Gut-derived sepsis occurs when the right pathogen with the right virulence genes meets the right host: evidence for in vivo virulence expression in Pseudomonas aeruginosa. *Ann Surg* 232:480–489.
22. Bertrand X, et al. (2001) Endemicity, molecular diversity and colonisation routes of Pseudomonas aeruginosa in intensive care units. *Intensive Care Med* 27:1263–1268.
23. Krol E, Becker A (2004) Global transcriptional analysis of the phosphate starvation response in Sinorhizobium meliloti strains 1021 and 2011. *Mol Genet Genomics* 272:1–17.
24. Hirsch J, et al. (2006) Phosphate deficiency promotes modification of iron distribution in Arabidopsis plants. *Biochimie* 88:1767–1771.
25. Lepine F, Deziel E, Milot S, Rahme LG (2003) A stable isotope dilution assay for the quantification of the Pseudomonas quinolone signal in Pseudomonas aeruginosa cultures. *Biochim Biophys Acta* 1622:36–41.